Predicting Organic-Inorganic Aerosol Efflorescence Using Thermodynamically Modeled Viscosity

Shanshan Chen[1], Qishen Huang[1*], Ying Li[2,3], Shu-Feng Pang[1], Pai Liu[1], Yun-Hong Zhang[1]

[1] State Key Laboratory of Environment Characteristics and Effects for Near-space, School of Chemistry and Chemical Engineering, Beijing Institute of Technology, Beijing, 100081, China

[2] School of Environmental Science and Technology, Dalian University of Technology, Dalian, 1116024, China

[3] Key Laboratory of Atmospheric Environment and Extreme Meteorology, Institute of Atmospheric Physics, Chinese Academy of Sciences, Beijing 100029, China

Abstract. Atmospheric aerosols, especially internally mixed organic-inorganic aerosols, exhibit complex phase behaviors that affect their size evolution, optical properties, and chemical reactivity, ultimately impacting climate and human health. Although parameterizations for secondary organic aerosol phase state exist, predictive models based on primary predictors for efflorescence in organic-inorganic aerosols remain underdeveloped. In this study, we evaluated several chemical parameters, including equivalent O:C ratio, organic mass fractions, glass transition temperature (T_g), and viscosity (η), and identified aerosol viscosity as the primary predictor of efflorescence relative humidity (ERH) in internally mixed organic-inorganic aerosols. We developed a linear viscosity-ERH model based on ERH and $\log_{10}\eta$, which defines the boundary conditions for aerosol efflorescence when $\eta < 4.76\times10^2$ Pa·s. Additionally, we showed that efflorescence is inhibited when $\eta > 4.76\times10^2$ Pa·s. Validation using an independent dataset showed strong agreement between predicted and experimentally measured ERH ($R^2 = 0.95$). A multivariate regression model incorporating η and T_g improved prediction accuracy but was limited by T_g parameterization for complex organic-inorganic mixtures. Our findings highlight the role of aerosol viscosity in controlling efflorescence and emphasize the need to develop improved aerosol viscosity measurement techniques to better constrain aerosol phase transitions in atmospheric models.

1 Introduction

Atmospheric aerosols significantly influence climate and human health through both direct and indirect effects. They directly influence the energy balance by absorbing and scattering solar radiation and indirectly affect the climate by acting as cloud condensation nuclei (CCN), thereby altering cloud microphysical properties such as droplet size, lifetime, and optical characteristics. (Boreddy et al., 2014; Fan et al., 2010; Knopf and Alpert, 2023; Novo et al., 2021; Pöschl, 2005; Shrivastava et al., 2017; Smith et al., 2021) Among aerosol physicochemical properties, phase state (liquid, solid, or semi-solid) is particularly important, as it governs hygroscopicity, optical properties, and heterogeneous reactivity. (Fard et al., 2018; Freedman et al., 2024; Novo et al., 2021) Moreover, aerosol phase transition significantly affects viral activity during transmission. (Oswin et al., 2022) Consequently, aerosol phase states substantially impact climate, air quality, and human health. (Reid et al., 2018)

Atmospheric aerosols, particularly internally mixed secondary aerosols composed of organic and inorganic components, exhibit diverse phase states, including liquid, liquid-liquid phase-separated, semi-solid, amorphous solid, and crystalline solid, which govern their physicochemical properties. (Novo et al., 2021) For instance, aerosols undergoing efflorescence (i.e., crystallization) and deliquescence exhibit hysteresis in particle size and water content in response to relative humidity (RH) variations. (Choi and Chan, 2002; Guo et al., 2020) In contrast, amorphous organic aerosols generally do not exhibit the pronounced discontinuous hysteresis associated with efflorescence and deliquescence of crystalline particles. However, semi-solid or glassy amorphous particles may still show gradual, kinetically driven hysteresis in water uptake and release because of slow diffusion and equilibration. (Koop et al., 2011) Thus, effloresced (or crystallized) aerosols display fundamentally different hygroscopic behaviors from amorphous ones, introducing uncertainties in predicting mixing aerosol water uptake and particle size under varying RH conditions because phase transitions and kinetic limitations can lead to different water contents and growth factors during hygroscopic cycles. (Marcolli and Krieger, 2006; Mikhailov et al., 2009)

Aerosol particles consisting of more than a single phase may have crystalline as well as amorphous phases. It is important to note that, in internally mixed organic–inorganic aerosols, the onset of phase transitions such as deliquescence and efflorescence typically occur only in specific components rather than the entire particle. For example, crystalline inorganic salts or hydrates may undergo deliquescence

or crystallization, while the remaining particle matrix can persist in an amorphous, semi-solid, or aqueous state. (Hodas et al., 2016)

However, internally-mixed organic-inorganic aerosols are chemically complex, often containing thousands of distinct organic species, of which only about 10% have been identified. (Hallquist et al., 2009) This limited chemical characterization constrains our ability to accurately predict aerosol phase states. Existing parameterization models based on organic aerosol properties, such as molecular weight and oxygen-to-carbon ratio (O:C ratio) (Shiraiwa et al., 2017), elemental composition (DeRieux et al., 2018), and volatility (Li et al., 2020; Zhang et al., 2019) to predict the glass transition temperature (T_g) have been established to predict the viscosity and phase state of organic aerosols but these models typically neglect efflorescence. Consequently, current parameterizations fail to distinguish between crystalline and amorphous solid states of internally mixed organic-inorganic aerosols and overlook the hysteresis in particle size and water uptake during efflorescence-deliquescence cycles. This limitation introduces significant uncertainty in predicting aerosol size evolution and leads to biases in describing atmospheric aerosol phase behavior, hygroscopicity, and optical properties, ultimately affecting our understanding of atmospheric particle aging, CCN activation, as well as climate and health impacts.

While laboratory studies have provided substantial data on efflorescence in mixed organic-inorganic aerosols, a systematic understanding of the key factors that govern and predict efflorescence remains limited. (Cai et al., 2017; Ma et al., 2021b; Wang et al., 2017) Efflorescence is a kinetically-controlled process that requires overcoming a nucleation energy barrier. This process is influenced by several factors. Component diffusion controls the mobility of ions and molecules and therefore affects the rate at which crystalline nuclei can form and grow; higher viscosity generally suppresses diffusion and delays efflorescence. (Ji et al., 2017; Mikhailov et al., 2009) Chemical composition, including solute concentration, solubility, and vapor pressure, influences the degree of supersaturation and thus the thermodynamic driving force for crystallization. (Cohen et al., 1987; Gupta et al., 2015) In addition, molecular interactions within the particle phase can either facilitate or hinder the structural rearrangement required for nucleation, while interfacial properties such as surface tension affect the nucleation energy barrier by altering the energetic cost of forming a new phase interface. (Davis et al., 2015; Ma et al., 2021a; Mikhailov et al., 2009) Furthermore, thermodynamic constraints exists for efflorescence. Crystallization can only occur when the aqueous phase becomes supersaturated with respect to the relevant solid phase; otherwise, efflorescence is thermodynamically inhibited. Once supersaturation is

achieved, nucleation and crystal growth proceed through kinetically controlled processes. (Bouzidi et al., 2022; Marcolli and Krieger, 2006) The transition point, described by the efflorescence relative humidity (ERH), is therefore strongly influenced by these factors, which are modulated by the properties of organic components, and the hydration state of the inorganic salts. The O:C ratio is widely used as a parameter for organic compound polarity. (Yu et al., 2021) Previous studies have shown that increasing the mass fraction of organic compounds (ω_{org}), particularly with high-viscosity organics, can significantly alter mass transport processes, and thereby affect phase transition. (Parsons et al., 2004; Shiraiwa et al., 2013; Virtanen et al., 2010; Wang et al., 2017; Zobrist et al., 2011) Under such conditions, efflorescence may be kinetically suppressed because of limited molecular diffusion, causing aerosol particles to remain in an amorphous semisolid or glassy state; in this case, their phase-state evolution is more appropriately characterized with reference to the glass transition temperature (T_g). (Berkemeier et al., 2016; Koop et al., 2011; Song et al., 2016b; Tong et al., 2011) However, direct and reliable measurements of the viscosity of atmospheric aerosols under atmospherically relevant conditions remain challenging (Fitzgerald et al., 2016; Hosny et al., 2016), particularly because water uptake can continuously modify particle composition, phase state, and molecular mobility. (Sheldon et al., 2023; Zobrist et al., 2008) This has resulted in limited observational data and motivated the use of thermodynamic models, such as AIOMFAC, to predict the viscosity of organic–inorganic mixed aerosols. (Lilek and Zuend, 2022)

In this study, we develop a parameterization for predicting the ERH of organic-inorganic aerosols by integrating literature-reported ERH data, investigating different aerosol physicochemical parameters, focusing on aerosol viscosity (η) and the collective effect of O:C ratio, ω_{org}, and T_g. The established framework enhances our understanding of aerosol phase behavior and size change during hygroscopic cycles, offering valuable insights into atmospheric processes, such as gas-particle partitioning, heterogeneous chemistry, and cloud formation.

2 Methods

2.1 The dataset for the parameterization

We compiled aerosol ERH data from our previous studies and peer-reviewed literature identified through Web of Science using keywords: aerosol, hygroscopic, and efflorescence. All studies were laboratory-based, with ERH measured using IR spectroscopy (Braban and Abbatt, 2004; Cai et al., 2017; Ghorai et

al., 2014; Ji et al., 2017; Ma et al., 2021b; Shi et al., 2017; Wang et al., 2017; Wu, 2017; Xu et al., 2022), Raman spectroscopy (Chang, 2020; Hu et al., 2025; Ushijima et al., 2021; Wang, 2018; Yu et al., 2012), optical microscopy (Bertram et al., 2011; Huang et al., 2024; Parsons et al., 2004) or Hygroscopicity Tandem Differential Mobility Analyzer (HTDMA). (Laskina et al., 2015) In multicomponent organic–inorganic particles, multiple efflorescence relative humidities may exist due to different salts crystallizing at distinct RH levels, and efflorescence typically occurs over a RH range. In this study, "aerosol ERH" is defined as the mean value of this transition range, serving as a simplified but effective macroscopic parameter for the overall phase transition of the particle.

A total of 102 ERH data points for organic-inorganic mixture aerosols were collected: 66 ERH points for the training set (Table S1) and the remaining 36 points for the validation set (Table S2). The training set includes aerosol compositions containing 14 organic compounds (composed of C, H, and O) and 4 inorganic salts (ammonium sulfate, ammonium nitrate, sodium chloride, and potassium chloride) mixed in varying ratios. All ERH data in the training were from our previous studies, and all corresponding viscosity data were derived using the AIOMFAC model. The particles investigated in our previous studies typically range from 1 to 10 μm in diameter. The validation set contains 36 ERH data from systems involving 12 organic compounds and 4 inorganic salts (Table S2), selected from studies that either reported both aerosol ERH and viscosity or observed no efflorescence. For dataset included in this study, experiments were conducted over several hours with slow RH change rate (< 0.1%/s) to ensure near-equilibrium conditions. Although these timescales are shorter than typical atmospheric aerosol lifetimes (days to weeks), previous studies have shown that nucleation induction times in high-viscosity systems can be extremely long due to diffusion limitations. (Wang et al., 2017) Therefore, the suppression of efflorescence at high viscosity reported in the cited studies is likely a fundamental kinetic constraint rather than an artifact of limited experimental duration. Moreover, the empirical data utilized to derive the regression model in this study were all obtained within a temperature range of 298 ± 10 K.

Key physicochemical parameters for predicting aerosol ERH include the equivalent O:C ratio of the mixture

$$\mathrm{O{:}C_{mixture}} = \left(\frac{n_{\mathrm{O,org}}}{n_{\mathrm{C,org}}}\right) \cdot x_{\mathrm{org}} \quad (1)$$

where x_{org} is the organic molar fraction.

$$x_{org} = \frac{n_{org}}{n_{org} + n_{inorg}} \quad (2)$$

and n_{inorg}=0 mol for purely organic aerosols (making $O:C_{mixture}$=O:C). Other parameters include ω_{org}, fractional T_g at ERH ($T_{g(\omega org)}$), and viscosity.

2.2 AIOMFAC model

Aerosol viscosity at the corresponding ERH and 298 K was estimated using the Aerosol Inorganic-Organic Mixtures Functional Groups Activity Coefficients (AIOMFAC) model. (Zuend et al., 2008, 2011) AIOMFAC is a thermodynamics-based group-contribution framework developed for aqueous organic-inorganic mixtures. To predict the viscosity of complex organic-inorganic mixtures, the AIOMFAC-VISC framework conceptually divides the mixture into two distinct sub-systems. For the aqueous inorganic (electrolyte) sub-system, it employs a semi-empirical model based on Eyring's absolute rate theory, which relates viscosity to the molar Gibbs energy of activation for viscous flow (Δg^*) taking into account temperature, ion activities, and ionic strength. Conversely, for the aqueous organic sub-system, the model relies on a combinatorial-activity-weighted approach based on functional group contributions. (Gervasi et al., 2020) Adopting the UNIFAC concept, AIOMFAC segments organic molecules into functional subgroups, treating the liquid mixture as a 'solution of groups' to manage chemical complexity. (Fredenslund et al., 1975; Hansen et al., 1991) In our study, the viscosity of mixed organic-inorganic phases was estimated using the default "aquelec" (electrolyte-aware water) approach in AIOMFAC-web. This method represents the effects of ions by first computing the viscosity of the aqueous electrolyte mixture (excluding organics), and then using that sub-system's viscosity to represent a modified viscosity of water in the calculation of the electrolyte-free organic sub-system. Validation against experimental data (e.g., Figure 11 in Lilek and Zuend et al.) has demonstrated that the aquelec approach accurately characterizes the viscosity of internally mixed aerosols such as sucrose-nitrate systems, establishing it as a robust tool for our predictions. (Lilek and Zuend, 2022; Song et al., 2021; Zuend et al., 2011) Validation against experimental viscosity data for sucrose–nitrate systems demonstrated that the aquelec approach accurately characterizes the viscosity of internally mixed organic–inorganic aerosols, establishing AIOMFAC-VISC as a robust tool for predicting atmospheric aerosol viscosity when experimental measurements are unavailable. (Lilek and Zuend, 2022)

Accordingly, viscosity calculations were performed by specifying the functional groups of the organic

components, inorganic salt composition, organic-to-inorganic ratio (OIR, molar ratio of organic compounds to inorganic salts, excluding water), and a series of organic molar fractions in the solute mixture, x_{org}, where the solute consists of organic compounds and inorganic salts, ranging from 0.01 to 0.99 in increments of 0.01. For each system, the viscosity corresponding to the water activity closest to the literature reported ERH (within ±0.5% RH) was selected. For example, in a 1,2,6-hexanetriol and ammonium sulfate (1:1) mixture, we defined 1,2,6-hexanetriol as 2 CH_2(OH), 1 CH(OH), 1 C and 3 OH. The viscosity of the mixture system was evaluated at a water activity of 0.47, which closely matches the ERH value in the literature (47.4%). Functional group definitions for all organic components are listed in Table S3. To assess the uncertainty associated with the thermodynamic state predictions, the sensitivity of viscosity (±log10(η/[Pa.s]) was calculated for each mixture. This metric quantifies the variation in predicted viscosity resulting from a ±2% perturbation in aerosol water mass fraction and serves as a proxy for uncertainty related to compositional variability. The corresponding values are listed in Table S1.

2.3 Calculation of the fractional glass transition temperature ($Tg_{(\omega org)}$)

Multiple parameterizations exist for estimating the glass transition temperature (T_g) of organic compounds, utilizing predictors such as chemical structure, volatility, or melting point (T_m) (Armeli et al., 2023; Galeazzo and Shiraiwa, 2022; Koop et al., 2011; Li et al., 2020). Recent machine-learning models based on chemical structure do not strictly require T_m information, though including it as an optional parameter can further improve predictive accuracy. (Armeli et al., 2023) The framework proposed by Armeli et al. comprises four distinct modes, contingent upon the specific input parameters available for a given compound: the Functional Group Mode (FGM) and the SMILES Mode (SM). Each mode features a variant that includes melting temperature as an additional feature (FGM with T_m; SM with T_m) and a version that operates without it (FGM no T_m; SM no T_m). The T_g values and parameters calculated according to the methodology of Armeli et al. are summarized in Tables S4 – S7.

The volatility-based parameterization developed by Li et al. (Eq. 3) predicts T_g from the saturation mass concentration (C^0).

$$T_g = 288.7 - 15.33 \times \log_{10}(C^0) - 0.33 \times [\log_{10}(C^0)]^2 \quad (3)$$

C^0 was estimated as a function of C, O, N, S numbers of the organic compound ($\log_{10}C^0 = f(n_C, n_O, n_N, n_S)$, Eq. 4) (Donahue et al., 2011; Li et al., 2016) :

$$\log_{10} C^0 = (n_C^0 - n_C)b_C - n_O b_O - 2\frac{n_C n_O}{n_C + n_O} b_{CO} - n_N b_N - n_S b_S. \quad (4)$$

Here, n_C^0 is the reference carbon number; n_C, n_O, n_N, and n_S denote the number of carbon, oxygen, nitrogen, and sulfur atoms, respectively; b coefficients (b_C, b_O, b_N, and b_S) denote atomic contributions fitted via multi-linear least squares analysis from 30,000 compounds across multiple classes (CH, CHO, CHN, CHON, CHOS, and CHONS). (Li et al., 2016) $b_{(CO)}$ represents the carbon-oxygen nonideality.

A comparison between the experimentally measured T_g values of the organic compounds and the predictions derived from the methods of both Li et al. (Li et al., 2020) and Armeli et al. (Armeli et al., 2023) is presented in Table S7.

The presence of inorganic salts (e.g., sodium nitrate) has been demonstrated to modulate the T_g of organic–inorganic mixtures; specifically, depending on the effective T_g of inorganic salt, the T_g of the mixture can be either elevated or depressed. (Dette and Koop, 2015) Typically, the T_g of organic–inorganic mixtures is calculated using the Gordon–Taylor equation (Gordon and Taylor, 1952):

$$T_g = \frac{\omega_1 T_{g1} + \frac{1}{k}\omega_2 T_{g2}}{\omega_1 + \frac{1}{k}\omega_2} \quad (5)$$

where T_g represents the glass transition temperature of the dry binary mixture, T_{g1} and T_{g2} are the T_g values of the respective pure compounds, ω_1 and ω_2 denote the mass fractions of the two components, and k is the Gordon–Taylor constant. However, the glass transition temperature of inorganic compounds is limited, we thus employ the glass transition temperature of the organic-water system ($T_{g,org\text{-}water}$) as a proxy for the overall mixture T_g when analyzing the correlation between efflorescence relative humidity (ERH) and T_g. In Eq. (5), the parameters ω_2 and T_{g2} are substituted with the mass fraction ω_{org} and the glass transition temperature $T_{g(\omega_{org})}$ of the organic component, respectively, where ω_{org} is the organic mass fraction calculated via the AIOMFAC model at aerosol ERH. $T_{g,w}$ is the glass transition temperature of pure water (136 K) (Kohl et al., 2005), while k_{GT} (the Gordon–Taylor constant) is assumed to be 2.5 for organic–water mixtures. (Koop et al., 2011; Zobrist et al., 2008) These two values are substituted for T_{g1} and k in the equation, with ω_1 calculated as (1-ω_{org}). As reported by Koop et al. (Dette and Koop, 2015), the T_g of $NaNO_3$ is specified as 290 K. Using this reported T_g value for $NaNO_3$ together with k_{GT} = 0.5, we calculated the T_g for dry glycerol/$NaNO_3$ and dry sucrose/$NaNO_3$ mixtures across a range of mixing ratios. (Figure S1) It should be noted that assuming a constant Gordon-Taylor parameter (k_{GT} = 2.5) for all organic–water mixtures represents a generalized simplification. The k_{GT} value essentially

parameterizes the interaction strength between water and the specific organic solute. Consequently, for organic mixtures with highly complex or varying oxygenated functional groups, the actual k_{GT} value may deviate from this assigned average (typically estimated within a range of 2.5 ± 1.0). This variability introduces a potential, albeit minor, source of uncertainty into the T_g-based model predictions presented in this study.

In addition to the approach used here for estimating $Tg(\omega_{org})$, the glass transition temperature of the entire mixture, including contributions from inorganic ions, could also be derived from the predicted mixture viscosity. This can be achieved by combining AIOMFAC-VISC viscosity predictions with an assumed fragility parameter within the Vogel–Tammann–Fulcher framework. (DeRieux et al., 2018) However, the pure-component viscosity parameterization for organics implemented in AIOMFAC-web may be less accurate than more recent approaches. (Armeli et al., 2023) Moreover, for the purposes of the present regression model, estimating T_g from mixture viscosity is likely redundant, as it does not provide additional predictive power beyond viscosity itself.

3 Results and Discussion

3.1 Correlation between ERH and physicochemical parameters

In the study of ERH presented here, we focus on the efflorescence of the inorganic component in internally mixed organic-inorganic aerosols. Therefore, we examined the correlation between ERH and key physicochemical parameters describing the organic components in organic-inorganic mixture aerosols: O:C ratio, ω_{org}, and $T_g(\omega_{org})$ (Figure 1).

Linear regression analysis using the training set (66 data points) showed no significant correlations between aerosol ERH and any of O:C, ω_{org}, or $T_g(\omega_{org})$ individually ($R^2 < 0.15$; Table S8). Multivariate regression considering the combined influence of three parameters provided only a limited improvement ($R^2 = 0.25$, Table S9). According to the nested cross-validated model evaluation reported by Armeli et al. (Armeli et al., 2023) for the full dataset, the SMILES mode with T_m showed the highest predictive accuracy among the four modes. Therefore, the T_g values calculated using the SMILES mode with T_m were selected for comparison with the parameterization developed by Li et al. (Li et al., 2020). The results, presented in Figure 1c, demonstrate that neither methodology yields a statistically significant correlation. Furthermore, analyses employing alternative FGM and SMILES models for T_g estimation, and T_g values for organic-inorganic mixtures were also investigated (Figure S2). Similarly, no discernible

correlation with ERH was observed.

When we color-coded the training dataset in Figure 1b-1d based on aerosol viscosity (the logarithm of viscosity estimated using the AIOMFAC, $\log_{10}\eta$), a clear trend emerged: aerosols with lower viscosity generally exhibited higher ERH, while those with higher viscosity tended to have lower ERH. This trend is further supported by the scatter plot of aerosol ERH versus viscosity (Figure 1a), which shows an apparent negative correlation. These results indicate that viscosity may play a key regulatory role in aerosol efflorescence and could be a critical predictor for ERH.

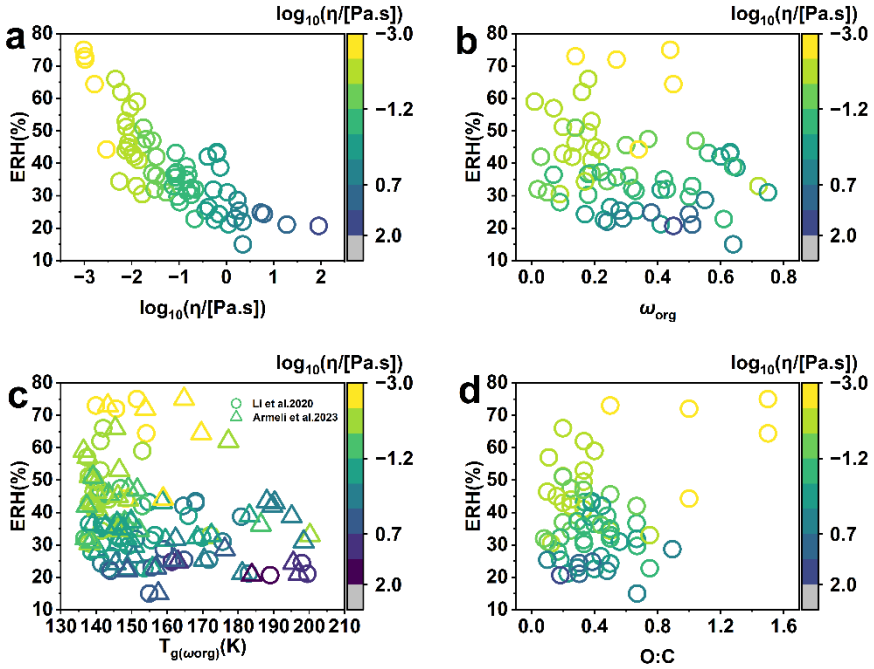

Figure 1. Relationships between the ERH of organic-inorganic mixed aerosols. (a) the logarithm of viscosity ($\log_{10}(\eta/[\mathrm{Pa}\cdot\mathrm{s}]$)), (b) the organic mass fraction (ω_{org}), (c) the glass transition temperature ($T_g(\omega_{org})$, K) calculated using the methods of Li et al. (Li et al., 2020) and Armeli et al. (Armeli et al., 2023), respectively, and (d) O:C ratio. The color bar denotes the aerosol viscosity in $\log_{10}(\eta/[\mathrm{Pa}\cdot\mathrm{s}])$.

3.2 ERH prediction using viscosity

Building on the correlation between viscosity and ERH observed in Figure 1, we developed a linear regression model using the training set (Figure 2). The fitted equation is

$$ERH(\%) = (-10.23 \cdot \log_{10}(\eta/(Pa \cdot s)) + 27.40) \cdot 100\% \quad (6)$$

The R^2 of the linear fit is 0.65, which suggests a significant correlation between aerosol viscosity and aerosol ERH. This indicates that the influence of organic components on aerosol efflorescence is primarily mediated through their effect on the aerosol viscosity. Interestingly, we found that although

aerosol efflorescence occurs due to the crystallization of aqueous inorganic salt, the correlation between aerosol viscosity and the normalized aerosol ERH defined as ERH/ERH_{Ing} (where ERH_{Ing} is the efflorescence relative humidity of the corresponding inorganic salt system) was even weaker (R^2 = 0.59, Figure S3). Moreover, the linear fit for organic–ammonium sulfate systems exhibits a similar correlation between ERH and viscosity, with comparable R^2, slope, and intercept to those obtained for the full dataset (Figure S4). Since the AIOMFAC calculation accounts for inorganic salts, this result emphasizes that the overall aerosol viscosity plays a dominant role in governing efflorescence, overwhelming differences between individual inorganic salts.

Our linear model can predict whether nucleation and crystal growth will occur at a given RH, and whether hygroscopic hysteresis is expected between humidification and dehumidification cycles. Notably, the model predicts that aerosol ERH approaches zero when viscosity reaches 4.76×10^2 Pa·s, and the corresponding 95% confidence interval is [1.05×10^2, 3.24×10^3] Pa·s. We therefore infer that organic-inorganic aerosols with viscosities exceeding 4.76×10^2 Pa·s are unlikely to undergo efflorescence. The complete viscosity-ERH model is expressed as:

$$ERH(\eta) = \begin{cases} (-10.23 \cdot \log_{10}\eta + 27.4) \cdot 100\%, & \eta < 4.76 \times 10^2 \mathrm{Pa \cdot s} \\ 0, & \eta \geq 4.76 \times 10^2 \mathrm{Pa \cdot s} \end{cases} \quad (7)$$

It should be emphasized that the empirical data utilized to derive this regression model were obtained at a constant temperature of 298 K. Given the well-established temperature dependence of both ERH and viscosity, the applicability of the current model is limited to standard room temperature conditions (298 K). Extrapolating this model to broader temperature regimes would necessitate further temperature-specific calibrations. In addition, the ERH model presented here is an empirical parameterization based on experimentally reported mean ERH values; therefore, it is intended to capture the occurrence of efflorescence, rather than the full statistical distribution of crystallization events. The model uncertainty reflects the scatter of the experimental ERH data, the stochastic nature of nucleation, and the uncertainty in AIOMFAC-predicted viscosity. The current model is mainly applicable to internally mixed organic–inorganic aerosols containing ammonium sulfate, ammonium nitrate, sodium chloride, or potassium chloride, with organic components primarily consisting of water-soluble C, H, and O, containing compounds, such as dicarboxylic acids and sugars.

We further performed multivariate regression incorporating viscosity ($\log_{10}\eta$), equivalent O:C ratio, ω_{org}, and $T_g(\omega_{org})$ as independent variables. The four-variable model demonstrated an improved R^2 of 0.69,

which is significantly different from the ERH-viscosity model (Sig. F change < 0.05, Table S10) due to the major contribution of viscosity and T_g (ω_{org}) (both showed $p < 0.05$, Table S10). We therefore established a bivariate viscosity-T_g-ERH model, and the analysis of variance (ANOVA) showed a Sig. F change (0.685) much greater than 0.05 with the same R^2 of 0.69. This indicated that there was no significant difference between the viscosity-T_g-ERH model and the four-variable model (Table S11), and O:C and ω_{org} did not significantly improve predictive performance. The viscosity-T_g-ERH model is expressed as:

$$ERH(\eta, T_g) = \left(0.25 \cdot (T_g(\omega_{org})/K) - 12.58 \cdot \log_{10}(\eta/(Pa \cdot s)) - 13.28\right) \cdot 100\% \quad (8)$$

Although adding predictors typically increases the coefficient of determination (R^2) by capturing additional variance, the inclusion of $T_g(\omega_{org})$ improved R^2 by only 0.04. In contrast, the viscosity-ERH model retains strong predictive power, while requiring fewer assumptions, demonstrating broader applicability and greater robustness for predicting ERH across diverse internally mixed organic–inorganic aerosols.

Moreover, the viscosity-T_g-ERH model exhibits practical limitations. The $T_g(\omega_{org})$ does not account for the effects of inorganic salts due to the limited availability of apparent T_g values for inorganic components. As shown in Figure S1, we estimated the T_g of organic/$NaNO_3$ mixtures by incorporating the T_g of pure $NaNO_3$ into the Gordon-Taylor framework, using a k_{GT} value of 0.5 extrapolated from Dette and Koop. (Dette and Koop, 2015) The result indicates that, regardless of whether the T_g of pure inorganic salt or water is used, the calculated $T_g(\omega_{org})$ exhibits no apparent correlation with ERH.

We also note that other parameters, such as aerosol pH, can affect the ERH of organic/inorganic aerosol (Sun et al., 2023); however, to the best of our knowledge, no consistent trend has been established regarding the direction or magnitude of this effect, since the influence of pH is highly dependent on the specific organic composition. Given that the modeled viscosity accounts for organic functional groups, the influence of pH may be implicitly reflected within the overall model uncertainty. Future studies should incorporate more inorganic T_g data and systematically investigate pH effects to provide more accurate $T_g(\omega_{org})$ and pH values and better evaluate the role of both parameters in the viscosity-ERH relationship.

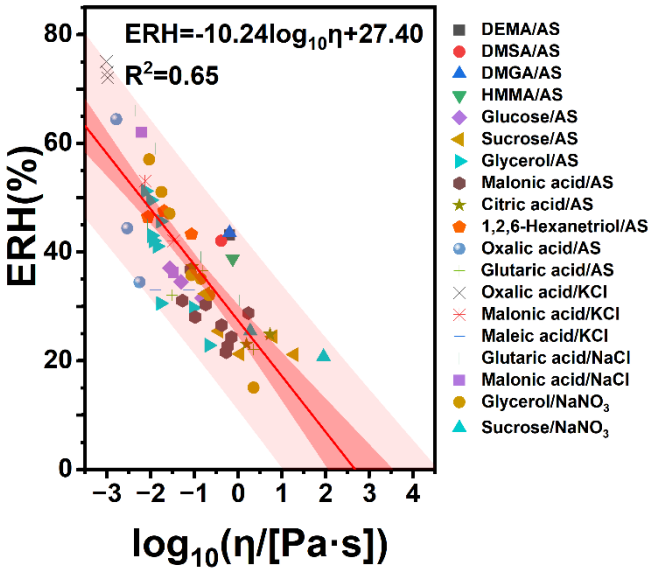

Figure 2. Linear fitting of aerosol ERH for different organic-inorganic aerosols by using viscosity ($\log_{10}\eta$) as the predictor. Data points are color- and shape-coded to distinguish between different organic and inorganic aerosol species. The red solid line represents the linear regression fit between viscosity and ERH. The dark pink band indicates the 95% confidence interval, while the light pink band shows the prediction interval. AS refers to ammonium sulfate, DEMA represents Diethyl malonic acid, DMSA represents 2,2-Dimethyl succinic acid, DMGA represents 3,3-Dimethyl glutaric acid, HMMA represents DL-4-Hydroxy-3-methoxymandelic acid and DHBA represents 2,5-Dihydroxybenzoic acid.

We then validated the established viscosity-ERH model using an independent validation set (32 data points) compiled from the literature. As depicted in Eq. (7), a threshold viscosity of 4.76×10^2 Pa·s distinguishes between crystallized and amorphous solid phases in atmospheric aerosols. Figure 3a compares the experimentally measured ERH in the validation set with model predictions. For viscosities $< 4.76\times10^2$ Pa·s (data points to the left of the red dashed line), all validation data fall within the predicted confidence intervals, confirming the reliability of using viscosity to predict the ERH of organic-inorganic mixture aerosols. This result suggests that when aerosol viscosity and ambient RH fall below the regression line (red), aerosols tend to undergo nucleation and crystal growth. For viscosities $> 4.76\times10^2$ Pa·s (data points to the right of the red dashed line), consistent with model predictions, aerosols in the validation set remain in a viscous liquid state and ultimately form amorphous solids without crystallization. As shown in Figure 3b, the data points tightly cluster around the y = x reference line (black dashed line), with the fitted line (red solid line) closely aligned and a slope near unity ($R^2 = 0.95$), indicating negligible systematic prediction bias and strong agreement between model predictions and experimental measurements. By performing the fitting analysis excluding the (0,0) data points (Figure S5), the slope remains close to unity, while the coefficient of determination decreases but remains

significant (R^2 = 0.68). We also validated the viscosity-T_g-ERH model using the same data set, excluding systems for which T_g could not be estimated. The viscosity-T_g-ERH model also demonstrated good agreement between predicted and measured ERH values (Figure S6).

To further elucidate the mechanistic basis of the model, we examined (i) viscosity changes for fixed chemical systems across RH (20 - 60%) and (ii) the correlation between viscosity at fixed RH and ERH. The slopes of the viscosity–RH relationships for representative systems range from -10 to -60 (Table S12), while the viscosity–ERH correlation weakens substantially when RH is held constant. These results indicate that the observed viscosity–ERH relationship primarily arises from the RH dependence of viscosity and confirm that efflorescence is governed by nucleation and crystal growth kinetics controlled by viscosity at the ERH. Accordingly, the viscosity–ERH model can be interpreted as a representative linear relationship that captures variability due to differences in organic composition and organic–inorganic interactions. It further defines a boundary condition for aerosol phase transitions: below the fitted viscosity–ERH line, aerosols tend to undergo efflorescence, whereas above this line (or beyond the threshold viscosity), aerosols tend to remain viscous without crystallization.

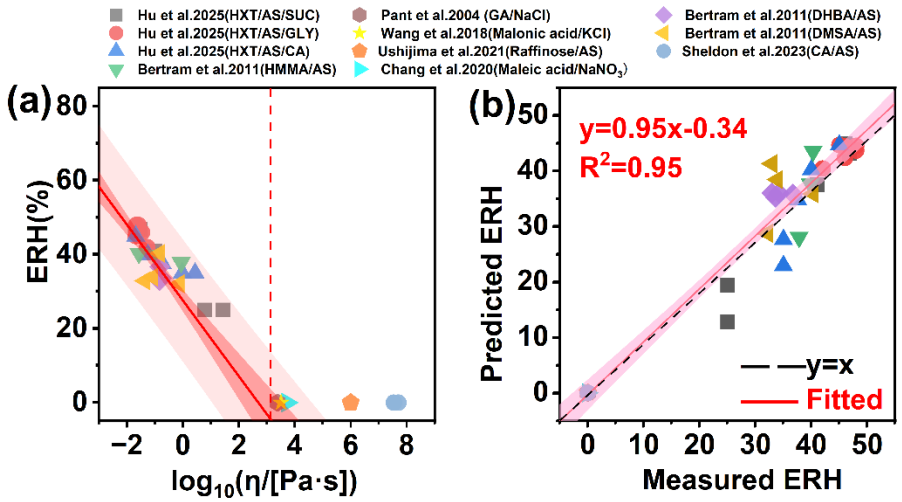

Figure 3. (a) Comparison between the validation set data and viscosity-ERH model prediction (Eq. 6). (b) Comparison of measured ERH values versus model predicted ERH values based on the viscosity-ERH model. The black dashed line denotes the y = x reference line, and the red line represents the linear regression fit to the data, along with the corresponding coefficient of determination, R^2=0.95. The pale pink shading represents the 95% confidence interval. DEMA represents Diethyl malonic acid, DMSA represents 2,2-Dimethyl succinic acid, DMGA represents 3,3-Dimethyl glutaric acid, HMMA represents DL-4-Hydroxy-3-methoxymandelic acid and DHBA represents 2,5-Dihydroxybenzoic acid, CA represents citric acid, SUC represents Sucrose, GA represents glutaric acid, HXT represents 1,2,6-hexanetriol.

3.3 Nucleation kinetics mechanism for viscosity-dependent ERH

Aerosol efflorescence is a kinetically controlled process involving: (1) formation of critical crystal nuclei in supersaturated droplets; (2) subsequent crystal growth, and (3) water evaporation. (Zhang et al., 2012) In highly viscous aerosols, mass transfer limitations significantly alter nucleation dynamics, making nucleus formation the rate-limiting step. (Ji et al., 2017; Wang et al., 2017) Turnbull and others showed that the nucleation rate can be expressed as the product of a pre-exponential factor and two thermally activated rate terms (Hollomon and Turnbull, 1953; Kelton et al., 1983; Turnbull, 1969):

$$\tau_x^{-1} = v \exp\left[\frac{-W(T)}{kT}\right] \exp\left[\frac{-\Delta G(T)}{kT}\right] \qquad (9)$$

where $W(T)$ represents the kinetic barrier associated with atomic rearrangement, and $\Delta G(T)$ is the thermodynamic free energy barrier for nucleus formation. The term $exp(W(T)/kT)$ represents the thermally activated atomic rearrangement rate (i.e., atomic mobility) in liquids and is inversely related to viscosity (η^{-1}). Here, we introduce an approximate proportional relationship between the kinetic barrier term and the logarithm of viscosity:

$$\frac{-W(T)}{kT} = -A log_{10}\eta \qquad (10)$$

where A is a constant linking $-W(T)/kT$ with $-log_{10}\eta$. Substituting this relation into Eq. (9) and taking $\log_{10}$ gives:

$$log_{10}(\tau_x^{-1}) = -A\log_{10}\eta + log_{10}v - \frac{\Delta G(T)}{2.303kT} \qquad (11)$$

The empirical relationship between ERH and aerosol viscosity (Eq.(6)) is consistent with Eq. 11, indicating that $\log_{10}\eta$ serves as a proxy for the kinetic energy barrier $W(T)$, while ERH reflects the effective nucleation rate. The intercept achieved in Eq.(6) can therefore be associated with $log_{10}v - \frac{\Delta G(T)}{2.303kT}$. Overall, the viscosity-ERH model parameterization aligns with this framework, showing that aerosol ERH decreases with increasing $log_{10}\eta$, corresponding to reduced atomic rearrangement rates. Since ambient RH governs aerosol water activity (a_w), the strong correlation between ERH and aerosol viscosity indicates that water activity and molecular mobility jointly control inorganic salt crystallization. Under low water activity, elevated viscosity suppresses molecular rearrangement, hinders nucleus formation, reduces nucleation rates, and consequently suppress or inhibits efflorescence. At this critical

viscosity threshold, the aerosol transitions from a liquid to a semi-solid phase, creating an immense kinetic barrier to molecular diffusion. Consequently, the nucleation induction time is prolonged so significantly that efflorescence is effectively inhibited, even over the extended residence times typical of aerosols in the atmosphere (days to weeks).

Thermodynamics-based approaches, such as that described by Hodas et al. (Hodas et al., 2016), predict salt crystallization and ERH based on the degree of supersaturation relative to the ion activity product (IAP). These frameworks capture the fundamental requirement that crystallization can only occur when the aqueous phase becomes thermodynamically supersaturated with respect to the relevant solid phase.

In this study, we consider aerosol conditions near ERH, where particles are expected to exhibit high ionic strength due to reduced water content. Under these conditions, we evaluate aerosol viscosity and its influence on phase transitions. Efflorescence is therefore interpreted as a coupled thermodynamic–kinetic process: while supersaturation provides the necessary driving force for crystallization, the actual onset of efflorescence is modulated by kinetic barriers associated with nucleation and crystal growth. In this context, aerosol viscosity plays a key role by limiting molecular diffusion and ion mobility.

Thus, thermodynamic and kinetic perspectives are complementary: thermodynamic conditions determine whether crystallization is possible, whereas viscosity provides a practical proxy for the kinetic limitations that govern when crystallization occurs.

While our results demonstrate a clear empirical correlation between viscosity and ERH, it is crucial to acknowledge that predicting ERH solely based on bulk viscosity has inherent limitations. As highlighted by previous studies (Ciobanu et al., 2010; Kuwata and Martin, 2012), in complex organic-inorganic systems, liquid-liquid phase separation (LLPS) frequently occurs, forming core-shell morphologies. In such core-shell aerosols, the inner aqueous inorganic-rich phase may maintain a low, liquid-like viscosity comparable to that of pure inorganic droplets, yet still exhibit a suppressed ERH. This suppression can arise because the organic coating alters the interfacial energy or acts as a physical barrier, independent of the inner core's viscosity. (Ciobanu et al., 2010) Therefore, while bulk viscosity acts as a critical kinetic constraint, the observed ERH is ultimately governed by a complex interplay of particle size, phase morphology, and viscosity.

4 Conclusions and Implications

Our results demonstrate that viscosity is a critical parameter governing aerosol phase-transition kinetics.

Although the model incorporating both viscosity and T_g improves explanatory power, the viscosity-ERH model developed herein offers broader applicability for complex atmospheric aerosols, providing a more practical framework for predicting aerosol phase behavior. According to the viscosity-ERH model, efflorescence is completely suppressed when viscosity exceeds 4.76×10^2 Pa·s.

Regional viscosity predictions by Zhang et al. suggest that in southern and northeastern China (Zhang et al., 2024), SOA are predominantly liquid or have low viscosities ($<10^4$ Pa s); in central and northeastern China, SOA typically exhibit semi-solid viscosities (10^5 - 10^8 Pa s); while highly viscous or glassy SOA ($\eta > 10^8$ Pa s) are mainly present in the northwest. Although SOA viscosity may significantly increase by several orders of magnitude as water content (and consequently aerosol water activity) decreases (Hosny et al., 2016; Renbaum-Wolff et al., 2013; Saukko et al., 2012; Song et al., 2016a; Yli-Juuti et al., 2017), SOA tend to become more oxidized and internally mixed with secondary inorganic aerosols during atmospheric aging. This aging process significantly lowers the overall viscosity of SOA due to the greater hygroscopicity of more oxygenated organics and inorganic salts. (Dette and Koop, 2015) Consequently, in more developed and urbanized regions like southern and northeastern China, atmospheric aerosols are more likely to undergo efflorescence and crystallization, leading to hysteresis in aerosol size and water contents during humidification and dehumidification processes. From a broader atmospheric perspective, the implications of aerosol phase state should be considered on regional to global scales. Shiraiwa et al. (Shiraiwa et al., 2017) showed that SOA phase state varies strongly with relative humidity and temperature, with SOA in the planetary boundary layer being predominantly liquid in humid tropical and polar regions, semi-solid in mid-latitudes, and solid over dry lands, while SOA in the middle and upper troposphere are expected to be mostly glassy. The hysteresis induced by aerosol efflorescence has important implications for modeling aerosol size evolution, optical properties, and chemical reactivity.

It is important to note that the aerosol viscosities in this study were derived from thermodynamic model predictions, as in-situ measurement techniques for atmospheric aerosol viscosity remain largely unavailable. Although substrate-based methods—such as poke-flow cytometry and fluorescence lifetime imaging microscopy (FLIM)—have been successfully employed to determine SOA viscosity under laboratory conditions, substrate effects must be carefully considered. (Grayson et al., 2015; Hosny et al., 2013) This highlights an urgent need to develop techniques that can directly measure aerosol viscosity at a given RH in ambient environments and to validate viscosity-dependent phase transition predictions. Optical tweezers is a promising tool for quantitative viscosity measurements of levitated particles;

however, the technique requires further advancement to measure submicron organic aerosols in real atmospheric conditions. (Reid et al., 2014) Further quantitative evaluation is needed to assess the extent to which viscosity-based predictive tools for aerosol phase state influence simulations of climate and air quality.

Code and data availability

The data supporting this article have been included in the main text and as part of the Supplementary Information: Tables S1-S12, Fig. S1-S6.

Supplement

The supplement related to this article is available online at:

Author contributions

SC and QH analyzed and visualized the data and wrote the original draft. SC conducted the experiments and model calculations. QH created the original research framework. QH and YL reviewed and edited the paper. QH, PL, and YZ supervised the study. All authors discussed the results and contributed to the article editing.

Competing interests

The contact author has declared that neither they nor their co-author has any competing interests.

Acknowledgements

We gratefully acknowledge the foundational model developed by Dr. Andreas Zuend, which served as an essential tool for our viscosity calculations. We thank Dr. Ying Li for providing feedback on an earlier draft of the manuscript. We also thank Dr. Thomas Koop for assisting us on the T_g calculation. During the preparation of this work the authors used Generative Pretrained Transformer 4 (GPT-4) to detect and correct grammatical errors in the draft. After using this tool/service, the authors reviewed and edited the

content as needed and take full responsibility for the content of the publication.

Financial support

This study was supported by the National Natural Science Foundation of China (No. 22406010, 42127806, and 42075110)

References

Armeli, G., Peters, J.-H., and Koop, T.: Machine-Learning-Based Prediction of the Glass Transition Temperature of Organic Compounds Using Experimental Data, ACS Omega, 8, 12298–12309, https://doi.org/10.1021/acsomega.2c08146, 2023.

Berkemeier, T., Steimer, S. S., Krieger, U. K., Peter, T., Pöschl, U., Ammann, M., and Shiraiwa, M.: Ozone uptake on glassy, semi-solid and liquid organic matter and the role of reactive oxygen intermediates in atmospheric aerosol chemistry, Phys. Chem. Chem. Phys., 18, 12662–12674, https://doi.org/10.1039/C6CP00634E, 2016.

Bertram, A. K., Martin, S. T., Hanna, S. J., Smith, M. L., Bodsworth, A., Chen, Q., Kuwata, M., Liu, A., You, Y., and Zorn, S. R.: Predicting the relative humidities of liquid-liquid phase separation, efflorescence, and deliquescence of mixed particles of ammonium sulfate, organic material, and water using the organic-to-sulfate mass ratio of the particle and the oxygen-to-carbon elemental ratio of the organic component, Atmospheric Chemistry and Physics, 11, 10995–11006, https://doi.org/10.5194/acp-11-10995-2011, 2011.

Boreddy, S. K. R., Kawamura, K., Mkoma, S., and Fu, P.: Hygroscopic behavior of water-soluble matter extracted from biomass burning aerosols collected at a rural site in Tanzania, East Africa, Journal of Geophysical Research: Atmospheres, 119, 12,233-12,245, https://doi.org/10.1002/2014JD021546, 2014.

Bouzidi, H., Fayad, L., Coeur, C., Houzel, N., Petitprez, D., Faccinetto, A., Wu, J., Tomas, A., Ondráček, J., Schwarz, J., Ždímal, V., and Zuend, A.: Hygroscopic growth and CCN activity of secondary organic aerosol produced from dark ozonolysis of γ-terpinene, Science of The Total Environment, 817, 153010, https://doi.org/10.1016/j.scitotenv.2022.153010, 2022.

Braban, C. F. and Abbatt, J. P. D.: A study of the phase transition behavior of internally mixed ammonium sulfate - malonic acid aerosols, Atmospheric Chemistry and Physics, 4, 1451–1459, https://doi.org/10.5194/acp-4-1451-2004, 2004.

Cai, C., Luan, Y., Shi, X., and Zhang, Y.: $(NH_4)_2SO_4$ heterogeneous nucleation and glycerol evaporation of $(NH_4)_2SO_4$-glycerol system in its dynamic efflorescence process, Chemical Physics, 483–484, 140–148, https://doi.org/10.1016/j.chemphys.2016.12.003, 2017.

Chang, P.: Study on single aerosol particle by spontaneous and stimulated Raman spectroscopy. Ph.D. Dissertation, Beijing Institute of Technology, 2020.

Choi, M. Y. and Chan, C. K.: The effects of organic species on the hygroscopic behaviors of inorganic aerosols, Environ. Sci. Technol., 36, 2422–2428, https://doi.org/10.1021/es0113293, 2002.

Ciobanu, V. G., Marcolli, C., Krieger, U. K., Zuend, A., and Peter, T.: Efflorescence of Ammonium

Sulfate and Coated Ammonium Sulfate Particles: Evidence for Surface Nucleation, J. Phys. Chem. A, 114, 9486–9495, https://doi.org/10.1021/jp103541w, 2010.

Cohen, M. D., Flagan, R. C., and Seinfeld, J. H.: Studies of concentrated electrolyte solutions using the electrodynamic balance. 3. Solute nucleation, J. Phys. Chem., 91, 4583–4590, https://doi.org/10.1021/j100301a031, 1987.

Davis, R. D., Lance, S., Gordon, J. A., Ushijima, S. B., and Tolbert, M. A.: Contact efflorescence as a pathway for crystallization of atmospherically relevant particles, Proc Natl Acad Sci U S A, 112, 15815–15820, https://doi.org/10.1073/pnas.1522860113, 2015.

DeRieux, W.-S. W., Li, Y., Lin, P., Laskin, J., Laskin, A., Bertram, A. K., Nizkorodov, S. A., and Shiraiwa, M.: Predicting the glass transition temperature and viscosity of secondary organic material using molecular composition, Atmospheric Chemistry and Physics, 18, 6331–6351, https://doi.org/10.5194/acp-18-6331-2018, 2018.

Dette, H. P. and Koop, T.: Glass Formation Processes in Mixed Inorganic/Organic Aerosol Particles, J. Phys. Chem. A, 119, 4552–4561, https://doi.org/10.1021/jp5106967, 2015.

Donahue, N. M., Epstein, S. A., Pandis, S. N., and Robinson, A. L.: A two-dimensional volatility basis set: 1. organic-aerosol mixing thermodynamics, Atmospheric Chemistry and Physics, 11, 3303–3318, https://doi.org/10.5194/acp-11-3303-2011, 2011.

Fan, J., Comstock, J. M., and Ovchinnikov, M.: The cloud condensation nuclei and ice nuclei effects on tropical anvil characteristics and water vapor of the tropical tropopause layer, Environ. Res. Lett., 5, 044005, https://doi.org/10.1088/1748-9326/5/4/044005, 2010.

Fard, M. M., Krieger, U. K., and Peter, T.: Shortwave radiative impact of liquid–liquid phase separation in brown carbon aerosols, Atmospheric Chemistry and Physics, 18, 13511–13530, https://doi.org/10.5194/acp-18-13511-2018, 2018.

Fitzgerald, C., Hosny, N. A., Tong, H., Seville, P. C., Gallimore, P. J., Davidson, N. M., Athanasiadis, A., Botchway, S. W., Ward, A. D., Kalberer, M., Kuimova, M. K., and Pope, F. D.: Fluorescence lifetime imaging of optically levitated aerosol: a technique to quantitatively map the viscosity of suspended aerosol particles, Phys Chem Chem Phys, 18, 21710–21719, https://doi.org/10.1039/c6cp03674k, 2016.

Fredenslund, A., Jones, R. L., and Prausnitz, J. M.: Group-contribution estimation of activity coefficients in nonideal liquid mixtures, AIChE Journal, 21, 1086–1099, https://doi.org/10.1002/aic.690210607, 1975.

Freedman, M. A., Huang, Q., and Pitta, K. R.: Phase Transitions in Organic and Organic/Inorganic Aerosol Particles, Annual Review of Physical Chemistry, 75, 257–281, https://doi.org/10.1146/annurev-physchem-083122-115909, 2024.

Galeazzo, T. and Shiraiwa, M.: Predicting glass transition temperature and melting point of organic compounds via machine learning and molecular embeddings, https://doi.org/10.1039/D1EA00090J, 2022.

Gervasi, N. R., Topping, D. O., and Zuend, A.: A predictive group-contribution model for the viscosity of aqueous organic aerosol, Atmospheric Chemistry and Physics, 20, 2987–3008, https://doi.org/10.5194/acp-20-2987-2020, 2020.

Ghorai, S., Wang, B., Tivanski, A., and Laskin, A.: Hygroscopic properties of internally mixed particles composed of NaCl and water-soluble organic acids, Environ. Sci. Technol., 48, 2234–2241, https://doi.org/10.1021/es404727u, 2014.

Gordon, M. and Taylor, J. S.: Ideal copolymers and the second-order transitions of synthetic rubbers.

i. non-crystalline copolymers, Journal of Applied Chemistry, 2, 493–500, https://doi.org/10.1002/jctb.5010020901, 1952.

Grayson, J. W., Song, M., Sellier, M., and Bertram, A. K.: Validation of the poke-flow technique combined with simulations of fluid flow for determining viscosities in samples with small volumes and high viscosities, Atmospheric Measurement Techniques, 8, 2463–2472, https://doi.org/10.5194/amt-8-2463-2015, 2015.

Guo, Y., Wang, N., Pang, S., and Zhang, Y.: Hygroscopic properties and compositional evolution of internally mixed sodium nitrate-amino acid aerosols, Atmospheric Environment, 242, 117848, https://doi.org/10.1016/j.atmosenv.2020.117848, 2020.

Gupta, D., Kim, H., Park, G., Li, X., Eom, H.-J., and Ro, C.-U.: Hygroscopic properties of NaCl and $NaNO_3$ mixture particles as reacted inorganic sea-salt aerosol surrogates, Atmospheric Chemistry and Physics, 15, 3379–3393, https://doi.org/10.5194/acp-15-3379-2015, 2015.

Hallquist, M., Wenger, J. C., Baltensperger, U., Rudich, Y., Simpson, D., Claeys, M., Dommen, J., Donahue, N. M., George, C., Goldstein, A. H., Hamilton, J. F., Herrmann, H., Hoffmann, T., Iinuma, Y., Jang, M., Jenkin, M. E., Jimenez, J. L., Kiendler-Scharr, A., Maenhaut, W., McFiggans, G., Mentel, T. F., Monod, A., Prévôt, A. S. H., Seinfeld, J. H., Surratt, J. D., Szmigielski, R., and Wildt, J.: The formation, properties and impact of secondary organic aerosol: current and emerging issues, Atmospheric Chemistry and Physics, 9, 5155–5236, https://doi.org/10.5194/acp-9-5155-2009, 2009.

Hansen, H. K., Rasmussen, P., Fredenslund, A., Schiller, M., and Gmehling, J.: Vapor-liquid equilibria by UNIFAC group contribution. 5. Revision and extension, Ind. Eng. Chem. Res., 30, 2352–2355, https://doi.org/10.1021/ie00058a017, 1991.

Hodas, N., Zuend, A., Schilling, K., Berkemeier, T., Shiraiwa, M., Flagan, R. C., and Seinfeld, J. H.: Discontinuities in hygroscopic growth below and above water saturation for laboratory surrogates of oligomers in organic atmospheric aerosols, Atmospheric Chemistry and Physics, 16, 12767–12792, https://doi.org/10.5194/acp-16-12767-2016, 2016.

Hollomon, J. H. and Turnbull, D.: Nucleation, Progress in Metal Physics, 4, 333–388, https://doi.org/10.1016/0502-8205(53)90020-3, 1953.

Hosny, N. A., Fitzgerald, C., Tong, C., Kalberer, M., Kuimova, M. K., and Pope, F. D.: Fluorescent lifetime imaging of atmospheric aerosols: a direct probe of aerosol viscosity, Faraday Discuss., 165, 343–356, https://doi.org/10.1039/C3FD00041A, 2013.

Hosny, N. A., Fitzgerald, C., Vyšniauskas, A., Athanasiadis, A., Berkemeier, T., Uygur, N., Pöschl, U., Shiraiwa, M., Kalberer, M., Pope, F. D., and Kuimova, M. K.: Direct imaging of changes in aerosol particle viscosity upon hydration and chemical aging, Chem. Sci., 7, 1357–1367, https://doi.org/10.1039/C5SC02959G, 2016.

Hu, S., Fan, R., Wu, L., Li, Y., Zhang, B., Yuan, Z., Li, Q., Ma, S., Zhao, Z., and Xu, T.: Influence of Amorphous Humic Acid Solids on the Phase Transition Behavior of Nitrate Aerosols, J. Phys. Chem. A, https://doi.org/10.1021/acs.jpca.5c03039, 2025.

Huang, Q., Pitta, K. R., Constantini, K., Ott, E.-J. E., Zuend, A., and Freedman, M. A.: Experimental phase diagram and its temporal evolution for submicron 2-methylglutaric acid and ammonium sulfate aerosol particles, Phys. Chem. Chem. Phys., 26, 2887–2894, https://doi.org/10.1039/D3CP04411D, 2024.

Ji, Z.-R., Zhang, Y., Pang, S.-F., and Zhang, Y.-H.: Crystal Nucleation and Crystal Growth and Mass Transfer in Internally Mixed Sucrose/NaNO3 Particles, J. Phys. Chem. A, 121, 7968–7975,

https://doi.org/10.1021/acs.jpca.7b08004, 2017.

Kelton, K. F., Greer, A. L., and Thompson, C. V.: Transient nucleation in condensed systems, J. Chem. Phys., 79, 6261–6276, https://doi.org/10.1063/1.445731, 1983.

Knopf, D. A. and Alpert, P. A.: Atmospheric ice nucleation, Nat Rev Phys, 5, 203–217, https://doi.org/10.1038/s42254-023-00570-7, 2023.

Kohl, I., Bachmann, L., Hallbrucker, A., Mayer, E., and Loerting, T.: Liquid-like relaxation in hyperquenched water at ≤140 K, Phys. Chem. Chem. Phys., 7, 3210–3220, https://doi.org/10.1039/B507651J, 2005.

Koop, T., Bookhold, J., Shiraiwa, M., and Pöschl, U.: Glass transition and phase state of organic compounds: dependency on molecular properties and implications for secondary organic aerosols in the atmosphere, Phys. Chem. Chem. Phys., 13, 19238–19255, https://doi.org/10.1039/C1CP22617G, 2011.

Kuwata, M. and Martin, S. T.: Phase of atmospheric secondary organic material affects its reactivity, Proc Natl Acad Sci U S A, 109, 17354–17359, https://doi.org/10.1073/pnas.1209071109, 2012.

Laskina, O., Morris, H. S., Grandquist, J. R., Qin, Z., Stone, E. A., Tivanski, A. V., and Grassian, V. H.: Size matters in the water uptake and hygroscopic growth of atmospherically relevant multicomponent aerosol particles, J. Phys. Chem. A, 119, 4489–4497, https://doi.org/10.1021/jp510268p, 2015.

Li, Y., Pöschl, U., and Shiraiwa, M.: Molecular corridors and parameterizations of volatility in the chemical evolution of organic aerosols, Atmospheric Chemistry and Physics, 16, 3327–3344, https://doi.org/10.5194/acp-16-3327-2016, 2016.

Li, Y., Day, D. A., Stark, H., Jimenez, J. L., and Shiraiwa, M.: Predictions of the glass transition temperature and viscosity of organic aerosols from volatility distributions, Atmospheric Chemistry and Physics, 20, 8103–8122, https://doi.org/10.5194/acp-20-8103-2020, 2020.

Lilek, J. and Zuend, A.: A predictive viscosity model for aqueous electrolytes and mixed organic–inorganic aerosol phases, Atmospheric Chemistry and Physics, 22, 3203–3233, https://doi.org/10.5194/acp-22-3203-2022, 2022.

Ma, S., Pang, S., Li, J., and Zhang, Y.: A review of efflorescence kinetics studies on atmospherically relevant particles, Chemosphere, 277, 130320, https://doi.org/10.1016/j.chemosphere.2021.130320, 2021a.

Ma, S., Chen, Z., Pang, S., and Zhang, Y.: Observations on hygroscopic growth and phase transitions of mixed 1, 2, 6-hexanetriol/$(NH_4)_2SO_4$ particles: investigation of the liquid–liquid phase separation (LLPS) dynamic process and mechanism and secondary LLPS during the dehumidification, Atmospheric Chemistry and Physics, 21, 9705–9717, https://doi.org/10.5194/acp-21-9705-2021, 2021b.

Marcolli, C. and Krieger, U. K.: Phase changes during hygroscopic cycles of mixed organic/inorganic model systems of tropospheric aerosols, J. Phys. Chem. A, 110, 1881–1893, https://doi.org/10.1021/jp0556759, 2006.

Mikhailov, E., Vlasenko, S., Martin, S. T., Koop, T., and Pöschl, U.: Amorphous and crystalline aerosol particles interacting with water vapor: conceptual framework and experimental evidence for restructuring, phase transitions and kinetic limitations, Atmospheric Chemistry and Physics, 9, 9491–9522, https://doi.org/10.5194/acp-9-9491-2009, 2009.

Novo, N., Carotenuto, A., Mensitieri, G., Fraldi, M., and Pugno, N.: Modeling of virus survival time in respiratory droplets on surfaces: a new rational approach for antivirus strategies, Frontiers in

Materials, 8, 631723, https://doi.org/10.3389/fmats.2021.631723, 2021.

Oswin, H. P., Haddrell, A. E., Otero-Fernandez, M., Mann, J. F. S., Cogan, T. A., Hilditch, T. G., Tian, J., Hardy, D., Hill, D. J., Finn, A., Davidson, A. D., and Reid, J. P.: Reply to Klein et al.: The importance of aerosol pH for airborne respiratory virus transmission, Proc Natl Acad Sci U S A, 119, e2212556119, https://doi.org/10.1073/pnas.2212556119, 2022.

Parsons, M. T., Knopf, D. A., and Bertram, A. K.: Deliquescence and crystallization of ammonium sulfate particles internally mixed with water-soluble organic compounds, J. Phys. Chem. A, 108, 11600–11608, https://doi.org/10.1021/jp0462862, 2004.

Pöschl, U.: Atmospheric aerosols: composition, transformation, climate and health effects, Angewandte Chemie International Edition, 44, 7520–7540, https://doi.org/10.1002/anie.200501122, 2005.

Reid, J. P., Power, R. M., Cai, C., and Simpson, S. H.: Micro-rheology and interparticle interactions in aerosols probed with optical tweezers, in: Optical Trapping and Optical Micromanipulation XI, Optical Trapping and Optical Micromanipulation XI, 258–264, https://doi.org/10.1117/12.2061018, 2014.

Reid, J. P., Bertram, A. K., Topping, D. O., Laskin, A., Martin, S. T., Petters, M. D., Pope, F. D., and Rovelli, G.: The viscosity of atmospherically relevant organic particles, Nat Commun, 9, 956, https://doi.org/10.1038/s41467-018-03027-z, 2018.

Renbaum-Wolff, L., Grayson, J. W., Bateman, A. P., Kuwata, M., Sellier, M., Murray, B. J., Shilling, J. E., Martin, S. T., and Bertram, A. K.: Viscosity of α-pinene secondary organic material and implications for particle growth and reactivity, Proceedings of the National Academy of Sciences, 110, 8014–8019, https://doi.org/10.1073/pnas.1219548110, 2013.

Saukko, E., Lambe, A. T., Massoli, P., Koop, T., Wright, J. P., Croasdale, D. R., Pedernera, D. A., Onasch, T. B., Laaksonen, A., Davidovits, P., Worsnop, D. R., and Virtanen, A.: Humidity-dependent phase state of SOA particles from biogenic and anthropogenic precursors, Atmospheric Chemistry and Physics, 12, 7517–7529, https://doi.org/10.5194/acp-12-7517-2012, 2012.

Sheldon, C. S., Salazar, J., Palacios Diaz, T., Morton, K., Davis, R. D., and Davies, J. F.: Correlating the Viscosity and Rate of Water Diffusion in Semisolid Gel-Forming Aerosol Particles, ACS Earth Space Chem., 7, 2311–2320, https://doi.org/10.1021/acsearthspacechem.3c00241, 2023.

Shi, X.-M., Wu, F.-M., Jing, B., Wang, N., Xu, L.-L., Pang, S.-F., and Zhang, Y.-H.: Hygroscopicity of internally mixed particles composed of (NH4)2SO4 and citric acid under pulsed RH change, Chemosphere, 188, 532–540, https://doi.org/10.1016/j.chemosphere.2017.09.024, 2017.

Shiraiwa, M., Zuend, A., Bertram, A. K., and Seinfeld, J. H.: Gas-article partitioning of atmospheric aerosols: interplay of physical state, non-ideal mixing and morphology, Phys. Chem. Chem. Phys., 15, 11441–11453, https://doi.org/10.1039/C3CP51595H, 2013.

Shiraiwa, M., Li, Y., Tsimpidi, A. P., Karydis, V. A., Berkemeier, T., Pandis, S. N., Lelieveld, J., Koop, T., and Pöschl, U.: Global distribution of particle phase state in atmospheric secondary organic aerosols, Nat Commun, 8, 15002, https://doi.org/10.1038/ncomms15002, 2017.

Shrivastava, M., Cappa, C. D., Fan, J., Goldstein, A. H., Guenther, A. B., Jimenez, J. L., Kuang, C., Laskin, A., Martin, S. T., Ng, N. L., Petaja, T., Pierce, J. R., Rasch, P. J., Roldin, P., Seinfeld, J. H., Shilling, J., Smith, J. N., Thornton, J. A., Volkamer, R., Wang, J., Worsnop, D. R., Zaveri, R. A., Zelenyuk, A., and Zhang, Q.: Recent advances in understanding secondary organic aerosol: Implications for global climate forcing, Reviews of Geophysics, 55, 509–559, https://doi.org/10.1002/2016RG000540, 2017.

Smith, J. N., Draper, D. C., Chee, S., Dam, M., Glicker, H., Myers, D., Thomas, A. E., Lawler, M. J., and Myllys, N.: Atmospheric clusters to nanoparticles: Recent progress and challenges in closing the gap in chemical composition, Journal of Aerosol Science, 153, 105733, https://doi.org/10.1016/j.jaerosci.2020.105733, 2021.

Song, M., Liu, P. F., Hanna, S. J., Zaveri, R. A., Potter, K., You, Y., Martin, S. T., and Bertram, A. K.: Relative humidity-dependent viscosity of secondary organic material from toluene photo-oxidation and possible implications for organic particulate matter over megacities, Atmospheric Chemistry and Physics, 16, 8817–8830, https://doi.org/10.5194/acp-16-8817-2016, 2016a.

Song, Y. C., Haddrell, A. E., Bzdek, B. R., Reid, J. P., Bannan, T., Topping, D. O., Percival, C., and Cai, C.: Measurements and Predictions of Binary Component Aerosol Particle Viscosity, J. Phys. Chem. A, 120, 8123–8137, https://doi.org/10.1021/acs.jpca.6b07835, 2016b.

Song, Y.-C., Lilek, J., Lee, J. B., Chan, M. N., Wu, Z., Zuend, A., and Song, M.: Viscosity and phase state of aerosol particles consisting of sucrose mixed with inorganic salts, Atmospheric Chemistry and Physics, 21, 10215–10228, https://doi.org/10.5194/acp-21-10215-2021, 2021.

Sun, J., Hu, Y., Cao, X., Pang, S.-F., Liu, P., Huang, Q., and Zhang, Y.-H.: Role of WSOCs and pH on Ammonium Nitrate Aerosol Efflorescence: Insights into Secondary Aerosol Formation, Environ. Sci. Technol., 57, 20074–20084, https://doi.org/10.1021/acs.est.3c07603, 2023.

Tong, H.-J., Reid, J. P., Bones, D. L., Luo, B. P., and Krieger, U. K.: Atmospheric Chemistry and Physics, 11, 4739–4754, https://doi.org/10.5194/acp-11-4739-2011, 2011.

Turnbull, D.: Under what conditions can a glass be formed?, Contemporary Physics, https://doi.org/10.1080/00107516908204405, 1969.

Ushijima, S. B., Huynh, E., Davis, R. D., and Tolbert, M. A.: Seeded crystal growth of internally mixed organic–inorganic aerosols: impact of organic phase state, J. Phys. Chem. A, 125, 8668–8679, https://doi.org/10.1021/acs.jpca.1c04471, 2021.

Virtanen, A., Joutsensaari, J., Koop, T., Kannosto, J., Yli-Pirilä, P., Leskinen, J., Mäkelä, J. M., Holopainen, J. K., Pöschl, U., Kulmala, M., Worsnop, D. R., and Laaksonen, A.: An amorphous solid state of biogenic secondary organic aerosol particles, Nature, 467, 824–827, https://doi.org/10.1038/nature09455, 2010.

Wang, L.-N., Cai, C., and Zhang, Y.-H.: Kinetically Determined Hygroscopicity and Efflorescence of Sucrose-Ammonium Sulfate Aerosol Droplets under Lower Relative Humidity, J Phys Chem B, 121, 8551–8557, https://doi.org/10.1021/acs.jpcb.7b05551, 2017.

Wang, X.: Study on the hygroscopicity of mixed aerosols composed of organic acids and inorganic salts by Raman spectroscopy.Ph.D. Dissertation, Beijing Institute of Technology, 2018.

Wu, F.: Thermodynamics and Kinetics Research of Mixed Inorganic/Glutaric acid Aerosols in the Hygroscopic Process.Ph.D. Dissertation, Beijing Institute of Technology, 2017.

Xu, Y., Liu, P., Ma, S., Pei, W., Pang, S., and Zhang, Y.: Efflorescence kinetics of aerosols comprising internally-mixed ammonium sulfate and water-soluble organic compounds, Atmospheric Environment, 274, 119007, https://doi.org/10.1016/j.atmosenv.2022.119007, 2022.

Yli-Juuti, T., Pajunoja, A., Tikkanen, O.-P., Buchholz, A., Faiola, C., Väisänen, O., Hao, L., Kari, E., Peräkylä, O., Garmash, O., Shiraiwa, M., Ehn, M., Lehtinen, K., and Virtanen, A.: Factors controlling the evaporation of secondary organic aerosol from α-pinene ozonolysis, Geophysical Research Letters, 44, 2562–2570, https://doi.org/10.1002/2016GL072364, 2017.

Yu, J.-Y., Zhang, Y., Zeng, G., Zheng, C.-M., Liu, Y., and Zhang, Y.-H.: Suppression of $NaNO_3$ Crystal Nucleation by Glycerol: Micro-Raman Observation on the Efflorescence Process of

Mixed Glycerol/$NaNO_3$/Water Droplets, J. Phys. Chem. B, 116, 1642–1650, https://doi.org/10.1021/jp210824e, 2012.

Yu, Z., Jang, M., and Madhu, A.: Prediction of phase state of secondary organic aerosol internally mixed with aqueous inorganic salts, J. Phys. Chem. A, 125, 10198–10206, https://doi.org/10.1021/acs.jpca.1c06773, 2021.

Zhang, R., Khalizov, A., Wang, L., Hu, M., and Xu, W.: Nucleation and growth of nanoparticles in the atmosphere, Chem. Rev., 112, 1957–2011, https://doi.org/10.1021/cr2001756, 2012.

Zhang, Y., Nichman, L., Spencer, P., Jung, J. I., Lee, A., Heffernan, B. K., Gold, A., Zhang, Z., Chen, Y., Canagaratna, M. R., Jayne, J. T., Worsnop, D. R., Onasch, T. B., Surratt, J. D., Chandler, D., Davidovits, P., and Kolb, C. E.: The Cooling Rate- and Volatility-Dependent Glass-Forming Properties of Organic Aerosols Measured by Broadband Dielectric Spectroscopy, Environ. Sci. Technol., 53, 12366–12378, https://doi.org/10.1021/acs.est.9b03317, 2019.

Zhang, Z., Li, Y., Ran, H., An, J., Qu, Y., Zhou, W., Xu, W., Hu, W., Xie, H., Wang, Z., Sun, Y., and Shiraiwa, M.: Simulated phase state and viscosity of secondary organic aerosols over China, Atmospheric Chemistry and Physics, 24, 4809–4826, https://doi.org/10.5194/acp-24-4809-2024, 2024.

Zobrist, B., Marcolli, C., Pedernera, D. A., and Koop, T.: Do atmospheric aerosols form glasses?, Atmospheric Chemistry and Physics, 8, 5221–5244, https://doi.org/10.5194/acp-8-5221-2008, 2008.

Zobrist, B., Soonsin, V., Luo, B. P., Krieger, U. K., Marcolli, C., Peter, T., and Koop, T.: Ultra-slow water diffusion in aqueous sucrose glasses, Phys. Chem. Chem. Phys., 13, 3514–3526, https://doi.org/10.1039/C0CP01273D, 2011.

Zuend, A., Marcolli, C., Luo, B. P., and Peter, T.: A thermodynamic model of mixed organic-inorganic aerosols to predict activity coefficients, Atmospheric Chemistry and Physics, 8, 4559–4593, https://doi.org/10.5194/acp-8-4559-2008, 2008.

Zuend, A., Marcolli, C., Booth, A. M., Lienhard, D. M., Soonsin, V., Krieger, U. K., Topping, D. O., McFiggans, G., Peter, T., and Seinfeld, J. H.: New and extended parameterization of the thermodynamic model AIOMFAC: calculation of activity coefficients for organic-inorganic mixtures containing carboxyl, hydroxyl, carbonyl, ether, ester, alkenyl, alkyl, and aromatic functional groups, Atmospheric Chemistry and Physics, 11, 9155–9206, https://doi.org/10.5194/acp-11-9155-2011, 2011.